Assessment of Muscle Fatigue using Sonomyography: Muscle Thickness Change Detected from Ultrasound Images

Jun Shi [1, 2] YP Zheng[1] X Chen[1] QH Huang[1]

[1] Department of Health Technology and Informatics, The Hong Kong Polytechnic University, Hong Kong

[2] School of Communication and Information Engineering, Shanghai University, Shanghai, China

Running Title:

Sonomyography Assessment for Muscle Fatigue

Corresponding Author:

Yongping Zheng, PhD

Department of Health Technology and Informatics,

The Hong Kong Polytechnic University,

Hung Hom, Kowloon, Hong Kong SAR, P.R.China

Tel: 852-27667664

Fax: 852-23624365

Email: ypzheng@ieee.org

Submitted to: **Medical Engineering and Physics**

Date of Submission**: Jan 17 06;** 1st revision: **May 5 06;** 2nd revision: **Jun 28 06**

Assessment of Muscle Fatigue using Sonomyography: Muscle Thickness Change Detected from Ultrasound Images

Jun Shi [1, 2] YP Zheng[1] X Chen[1] QH Huang[1]

[1]Department of Health Technology and Informatics, The Hong Kong Polytechnic University, Hong Kong

[2]School of Communication and Information Engineering, Shanghai University, Shanghai, China

Abstract: Muscle fatigue is an exercise-induced reduction in maximal voluntary muscle force. As the surface electromyography (SEMG) can be used to estimate the features of neuromuscular activations associated with muscle contractions, it has been widely employed as an objective tool to evaluate muscle fatigue. On the other hand, ultrasound imaging can inherently provide the morphological information of individual muscle, thus the architectural changes of muscles during fatigue can be obtained. In this study, we demonstrated the feasibility of using the dimensional change of muscles detected by ultrasound images, named as sonomyography (SMG), to characterize the behavior of muscles when they were in fatigue. The SEMG signals of the muscles were also recorded simultaneously and used for comparison. The right biceps brachii muscles of 8 normal young male adult subjects were tested for 30s under 80% of the maximal voluntary isometric contraction. The muscle fatigue was indicated by the change of the root-mean-square (RMS) and median frequency (MDF) of the SEMG signals. The results showed that the SEMG RMS had a linear increase with time with a rate of 2.9 ± 1.9 %/s (mean±SD), while the MDF decreased linearly with a rate of -0.60 ± 0.26 Hz/s. The muscle thickness, detected from the ultrasound images, continuously increased during the muscle fatigue but with a nonlinear increase with time, which was rapid during the initial 8.1 ± 2.1 s with a mean deformation rate of 0.30 ± 0.19 %/s and then became slower with a rate of 0.067 ± 0.024 %/s up to 20 s after the contraction. The muscle deformation at 20 s was 3.5 ± 1.6 %. The results demonstrated that the architectural change of muscles detected using SMG could potentially provide complementary information for SEMG for the muscle fatigue assessment.

Key Words: muscle fatigue, ultrasound, sonomyography, SMG, electromyography, EMG, mechanomyography, MMG

INTRODUCTION

Muscle fatigue, which is an exercise-induced reduction in maximal voluntary muscle force [1], frequently occurs in our daily life. It can be categorized into: 1) central fatigue, defined as a decline of alertness, mental concentration, motivation, and other psychological factors, and 2) peripheral fatigue defined as the changes in physiological processes [1]. Many methods have been developed to evaluate muscle fatigue, including oxygen uptake [2], heart rate [3], pH value of the muscle interstitial fluid [4], muscle generated force [5], muscle stiffness [6], surface electromyography (SEMG) [7][8], and invasive needle EMG [9], etc.

As muscle fatigue is an ongoing process during muscle activities rather than a failure at a time point, it is important to monitor the temporal changes of the physiological variables as the fatigue develops [8]. The SEMG signal, which contains the features of the neuromuscular activation associated with the muscle contraction, has been considered as an objective tool to evaluate muscle fatigue non-invasively. The root-mean-square (RMS) and median frequency (MDF) of SEMG are frequently used for the estimation of muscle fatigue. However, they are also sensitive to other factors which may change during the muscle contraction [10]. Alternative signals with the potential to tackle these challenges to SEMG are in demand and are being explored in the related fields. For example, mechanomyography (MMG) [12]-[14], which detects the sound or vibration generated by muscles during contraction, and near-infrared spectroscopy [13] have been used for the assessment of muscle fatigue.

Since early 1990's, sonography has been used to measure the changes in muscle thickness [15][16], muscle fiber pennation angle [17]-[20], muscle fascicle length [15][17]-[20], and muscle cross-sectional area [17][21] during isometric and dynamic contractions. As these architectural parameters have a close relationship with the muscle functions [22], they can be potentially used to characterize muscle activities during its contraction. Some researchers recently began to investigate the relationships between the ultrasound parameters and the EMG activities in quasi-static [15][23][24] and dynamic ways [25][26]. However, few studies have been conducted on muscles fatigue using both ultrasound and EMG signals. Only most recently, two papers which examined the muscle architecture with ultrasound during fatigue [25][26] were reported.

The aim of this study was to investigate the feasibility of using the muscle thickness change continuously extracted from the ultrasound images, named as sonomyography (SMG) [16], to characterize the muscle fatigue. The ultrasound and SEMG signals were collected simultaneously from the biceps brachii of 8 normal young male adult subjects under an isometric contraction. The SEMG parameters and the muscle deformation were calculated. The features of the muscle deformation signal during muscle fatigue were described and its potential contributions to the muscle fatigue evaluation were discussed.

SUBJECTS AND METHODS

Eight healthy male subjects participated in this study (age: 27 ± 3 years; height: 169 ± 3 cm; weight: 65 ± 5 kg). None of them had history of neuromuscular disorders and each gave written informed consent prior to the experiment.

The subject was seated comfortably on the adjustable chair of a Cybex machine (Cybex Norm Testing & Rehabilitation System, Cybex Norm Int. Inc., Ronkonkoma, USA) with the trunk of the body fixed by a strap to the chair back to restrict the posture change during the test. The forearm was placed and fixed on a forearm holder and the hand griped a vertical lever arm. The elbow was flexed at 90° with the upper arm vertical and the forearm oriented horizontal. The axis of the lever arm was mounted to be parallel with the rotational axis of the elbow joint. The hand was maintained in the halfway between pronation and supination. The right arm was chosen for measurements, which in all subjects was the dominant one.

After several warm-up contractions, three isometric maximal voluntary contractions (MVC) were performed by each subject at the beginning of the measurement. The subject was asked to produce the maximal isometric elbow flexion at 90° as the MVC. The real time visual feedback of the torque value was displayed on a computer screen. Each MVC lasted for approximately 3s with a rest interval of 60s between adjacent contractions. The MVC torque for each subject was defined as the mean of the maximum values of the torque generated during the three contractions.

When the experiment began, the subject was asked to perform an elbow flexion against the lever arm to the 80% of his MVC [27] and maintained this value through the visual feedback of the torque reading on the screen. The test was stopped when the torque dropped to approximately 70% of the MVC. The data collection for the torque, ultrasound image, and SEMG signal were started after the torque reached the 80% MVC. To maintain the subject's concentration, constant encouragement was given verbally during the contraction period. Usually, the endurance time did not exceed 30s for all the subjects. Totally three repeated voluntary contractions were performed at the same MVC level with a rest interval of at least 5 minutes [28][29] between adjacent contractions.

A dynamometer (Cybex Norm Testing & Rehabilitation System, Cybex Norm Int. Inc., Ronkonkoma, USA) was used to measure the elbow flexion torques. The torque signals from the dynamometer were amplified by a custom-made amplifier and digitized by a data acquisition card (NI PCI-6024E, National Instruments, Austin, USA) installed in the PC, where they were synchronized with the ultrasound images and SEMG signals. The experiment setup is shown in Fig. 1.

The ultrasound system used in this study was the same as that in a previous study on the potential of SMG for prosthesis control [16]. The sonography of a cross-sectional area of the biceps brachii was recorded using a portable B-mode ultrasound scanner (180 Plus, Sonosite Inc., Washington, USA) with a 7.5 MHz / 38 mm linear probe (L38, Sonosite Inc., Washington, USA). The depth of the device was 46 mm. Under this setting, the corresponding pixel resolution was approximately 0.1 mm in both x and y directions. According to the measurements using phantoms, the axial and lateral resolutions of the ultrasound image were 0.87 ± 0.13 mm, 0.92 ± 0.21 mm, respectively. The probe was fixed by a custom-made bracket and was perpendicular to the skin surface of the biceps brachii region with its image plane arranged vertically to the orientation of the biceps brachii muscle. The probe surface had a distance from the skin surface to avoid any compression on the tissue during the whole contraction period. Hence, the change of the muscle thickness was only contributed by the behaviors related to the muscle fatigue. Ultrasound gel was used to fill the gap between the probe and the skin to maintain a good coupling during the test. The video output of B-mode ultrasound scanner was digitized by a video capture card (NI PCI-1411, National Instruments, Austin, USA) with a sample rate of 8 Hz. The images were saved frame by frame together with other signals for subsequent analysis.

After cleaning the skin with alcohol, a pair of EMG biploar Ag-Agcl electrodes (Axon Systems, Inc., New York, USA) was placed between the transducer and the elbow joint and near the ultrasound probe along the orientation of the biceps brachii muscle. The distance between the two electrodes was approximately 20 mm. The EMG reference electrode was placed on the proximal head of the ulna. The EMG signal was amplified and filtered by a custom-made device with a gain of 10 and bandwidth of 10-800Hz and then digitized by the A/D card (NI PCI-6024E National Instruments, Austin, USA), which provided an additional gain of 10. The sample rate for colleting EMG was 4 kHz.

The data acquisition was controlled by a custom-developed program for the ultrasonic measurement of motion and elasticity (UMME) using Visual C++ 6.0 (Microsoft, Washington, USA) [16]. Multithread technology was applied in UMME software to insure the synchronization among the ultrasound image, torque, and SEMG. The ultrasound images were sampled frame by frame, each accompanied by an SEMG epoch of 125 ms and a torque value.

All the ultrasound, SEMG and torque signals were processed off-line using the UMME program and another program written in MATLAB (Version 6.5, MathWorks, Inc., Massachusetts, USA). The ultrasound images were imported to the UMME software and displayed frame by frame. A cross-correlation algorithm was used to track the displacements of the interested tissue regions in the images. It has been reported that the correlation tracking algorithm can work for images with low signal noise ratio (SNR) and with complex structures of target and background [30], and is particularly useful for the ultrasound images with complex speckles [16]. It requires a reference image or template (containing the interested object) from an initial image frame and looks for the most similar area to the reference image for estimating the object position in the updated frame [30][31]. In this study, two rectangular blocks were manually selected for the upper and lower boundaries of the cross-sectional image of the biceps brachii in the first frame of the image sequences (Fig. 2a). The images defined by these two blocks were regarded as two templates for the subsequent automatic tracking. The echoes reflected from the muscle-humerus interface were selected as the lower boundary of the elbow flexion muscles, which were mainly the biceps brachii with a small portion of brachialis (Fig. 2). These echoes were much easier to track in comparison with those from the fascia between the biceps brachii and the brachialis. The centers of the upper and lower template blocks were placed at the subcutaneous fat-muscle interface and the upper boundary of the humerus, respectively (Fig. 2a). The sizes of the blocks were selected manually to include enough features for a reliable tracking with a cross-correlation coefficient larger than 0.9 between two conjunctive frames. This manual selection of the blocks may slightly affect the value of the muscle thickness, but its effect on the deformation measurement can be negligible. Figure 2a was taken at the moment when the torque first reached 80% MVC and Fig. 2b at the moment when the torque started to decrease to below that level. The image correlation tracking algorithm was implemented in UMME software to track the movement of each selected block frame by frame both in vertical and horizontal directions [16]. The equation used to calculate the normalized two-dimensional cross-correlation is as follow:

$$R(i,j)=\frac{\sum_{m=0}^{M-1}\sum_{n=0}^{N-1}[x(m,n)-\bar{X}][y(m,n)-\bar{Y}]}{\sqrt{\sum_{m=0}^{M-1}\sum_{n=0}^{N-1}[x(m,n)-\bar{X}]^2\sum_{m=0}^{M-1}\sum_{n=0}^{N-1}[y(m+i,n+j)-\bar{Y}]^2}} \quad (1)$$

where $x(m,n)$ and $y(m+i,n+j)$ (*m=0, M, and n=0, N*) are the pixels of the selected image blocks in two different frames. The image block $x(m,n)$ is regarded as the template. The block represented by $y(m+i,n+j)$ shifts by *i* and *j* pixels in the horizontal and vertical directions, respectively, in comparison with the template represented by $x(m,n)$. $\bar{X}$ and $\bar{Y}$ represent the means of pixel density for the image blocks $x(m,n)$ and $y(m+i,n+j)$, respectively, while $R(i,j)$ is the cross-correlation coefficient between them. By changing *i* and *j*, the correlation coefficients between the template in the first image and a group of image blocks in the second image can be calculated. The best matched image block of the template can then be located according to the peak value of the correlation coefficients. In this study, the search range was set to be -10 to 10 pixels in the horizontal direction (*i*) and -40 to 40 pixels in the vertical direction (*j*), respectively. After finishing the matching for one frame, the template was automatically updated with the most similar image blocks, which might shift from the position of the initial template. After the initial template was manually selected, the above process would be automatically performed for each subsequent image frame until the last one and the positions of matched image blocks were recorded. It was demonstrated that the algorithm could achieve a resolution of 0.1 mm for the displacement measurement for tracking the selected image block, which was the same as the image pixel resolution.

The distance between the centers of the two image blocks was calculated for each frame, which was defined as the muscle thickness at each moment. The percentage deformation of the muscle was defined as:

$$\rho = \frac{(d - d_0)}{d_0} \times 100\% \qquad (2)$$

where d_0 is the initial muscle thickness at the moment when the subject first contracted to 80% MVC, d is the muscle thickness measured at each frame.

The RMS of amplitude and MDF of the SEMG signals were calculated for each epoch using the program written in MATLAB. The change rates of RMS and MDF as functions of the muscle contraction time were further calculated using linear regressions.

RESULTS

Figures 3a and 3b show the typical results of SEMG RMS and MDF for a trial on one subject. In Fig. 3a, the y-axis was normalized by the first RMS value for each trial. The results of other subjects showed similar trends. The increase of RMS and decrease of MDF as a function of time during the muscle fatigue were consistent with the results previously reported [7][32]-[34]. The changes of the SEMG parameters confirmed that the investigated muscles had experienced fatigue during the experiments. Figure 4a shows the increasing rate of SEMG RMS, and 4b the decreasing rate of MDF of different subjects, with the error bars representing the standard deviation (SD) of the three tests for each subject. The overall change rates of SEMG RMS and MDF of the 8 subjects were 2.9 $\pm$ 1.9 %/s (mean$\pm$SD) and -0.60 $\pm$ 0.26 Hz/s, respectively.

Figure 3c shows the muscle deformation of the same subject as in Figs. 3a and 3b. The muscle thickness increased obviously during the contraction, but in a complex nonlinear manner. Figure 5 shows the muscle deformations of all the 8 subjects at 20 s after the contraction. The overall mean deformation was 3.5 $\pm$ 1.6% at that moment. During the first several seconds after the contraction, the muscle thickness increased rapidly with a mean change rate of 0.30 $\pm$ 0.19 %/s for the 8 subjects (Fig. 6a). We defined this rate as the initial muscle deformation rate. It lasted for 8.1 ± 2.1 s (Fig. 6c), and then the muscle thickness increased gradually with a smaller change rate of 0.067 ± 0.024 %/s (Fig. 6b) till the moment of the torque fluctuation, which indicated that the subject could not maintain the assigned torque any more. We defined this lower rate as the steady muscle deformation rate. The transition time between the initial and steady muscle deformation rates was named as the critical time, which was calculated as the cross point of the two linear trend lines as shown in Fig. 3c. From Fig. 3c, we can find that the deformation reached a peak at the time of approximately 25s and then descended. This was because the subject could not maintain the 80% MVC anymore and the torque tended to fluctuate. For all the subjects, this phenomenon happened between 20 and 30 s of the experimental time. Interestingly, this fluctuating torque was not reflected in the corresponding RMS or MDF of the SEMG signals as shown in Figs. 3a and 3b.

The correlations between the muscle deformation and SMEG parameters were also investigated. The R^2 values of the linear regressions were all smaller than 0.3, indicating that no strong correlation could be observed between the muscle deformation and the SEMG parameters during the fatigue of the muscle.

DISCUSSION

We described a method to simultaneously collect the SEMG signals and ultrasound images of the biceps brachii muscle during an isometric contraction of the 80% MVC. From the SEMG signals, the RMS and MDF data were derived, while the muscle deformation was obtained from the ultrasound images, i.e. sonomyography

(SMG). It was confirmed that the muscles experienced fatigue according to the increase of RMS and the decrease of the MDF data [7][32]-[34]. It was also observed that the muscle thickness increased rapidly during the first several seconds, then increased gradually till the torque fluctuation, i.e. the subject could not maintain the 80% MVC. The transition of the muscle deformation rate might be explained as follow_using the recruitment pattern and firing rate of the motor units during muscle contraction.

In this study, the subject was asked to maintain a constant torque till he could not persist and the joint angle remained constant during the test. The “size principle” [35] suggested that more and more motor units might be recruited during the fatigue process in order to compensate the inability of the activated muscle fibers and to maintain their force generation [34]. According to the sliding filament theory of muscle contraction [36], the newly recruited fibers could locally shorten to generate enough force to maintain the torque. Consequently, the lateral dimension might increase at some local regions. Furthermore, it has recently been reported that the fascicle length significantly decreased and the pennation angle increased for the gastrocnemius medialis muscle in vivo during the process of sustained isometric contraction till fatigue [25]. The decreasing fascicle length and increasing pennation angle were accounted for the creep of the corresponding tendon during the sustained isometric contraction [25] and would result in the shortening of the muscle. According to Swammerdam’s result [37] that the muscle volume kept constant during contraction while the muscle shortening might cause the increase of muscle cross-sectional area as well the muscle thickness [38]-[40]. Therefore, our finding of the increasing muscle thickness during the sustained isometric contraction was consistent with the result of this recent study [25], though the muscles studied were different. Further studies should be followed to measure the creep of tendons and the dimensional change of their corresponding muscles simultaneously seeking a better explanation for the findings of the present study.

Interestingly, it was reported that the amplitude of the sound generated by the muscle (mechanomyogram, MMG) showed a significant increase during the initial phase of a sustained contraction and declined significantly when exhaustion was approached [12]. Their results may correlate with our findings in this study. The muscle sound is generated by the summation of the vibration of single motor unit during contraction [41]. Further studies are required to systematically investigate the mechanisms of the new findings observed in this study and the correlations among different types of signals generated during the muscle fatigue.

We could not observe any indication of the torque fluctuation or the transition phenomenon in the SEMG parameters (Fig. 3). The SEMG RMS and MDF linearly increased and decreased, respectively, as time going during the whole measurement even after the measured torque started to fluctuate. On the contrary, the results of muscle deformation clearly indicated the torque fluctuation. This might reflect the fact that the muscle deformation, similar to MMG, is a measure of actuation achieved (mechanical output), while the SEMG is a measure of activation intended (electrical input). As the muscle begins to fatigue, the neurons continue to fire at the same or greater rate trying to activate the fibers to maintain the force output which results in the continuous increase of the SEMG magnitude, but the fibers are unable to respond causing the torque fluctuation. There is dissociation between the electrical and mechanical activation of the muscle. Therefore, if we combine the information provided by the muscle deformation and SEMG signals together, the muscle fatigue can be potentially better characterized.

The subject number (n=8) is relatively small and only a specific group of subjects (normal young male adults) were tested in this study. Since ultrasound imaging can inherently provide the morphological information of individual muscles, it should have potential to assess the fatigue of overlapped muscles. It has been reported that the MMG parameters of biceps brachii and soleus muscles were significantly different during the sustained isometric contraction [12]. Further investigations with diverse and a larger number of subjects on different types of muscles are required to confirm the potential applications of SMG for the fatigue analysis, particularly its capability of differentiating neighboring deep muscles. It was noted that the variations of the muscle deformation and SEMG parameters among the three repeated tests were similar. For some subjects, the variations were relatively large. Therefore, it is necessary to understand better in future studies what affects the extraction of the parameters.

In this study, we used two rectangular blocks to automatically track the selected upper and lower boundaries of the muscle for the sequence of real-time ultrasound images using cross-correlation algorithm. The automatic correlation tracking was performed for the image translating but not for rotation. It is possible that there is rotational movement between the skin and the bone references during the muscle contraction, particularly during the process of isometric or isotonic contractions. The rotation of the muscle bundles was obvious during the process to reach the torque of 80% MVC, but not when a constant torque level was maintained. As described earlier, all the data were collected after the torque reached 80% MVC, so the rotation should have had minimal effect on the results. This could be confirmed by the high correlation coefficient ($R > 0.9$) of the cross-correlation tracking for the skin reference and the bone reference among the image frames collected during the fatigue process. If a significant rotation happened for the tracking references, the correlation coefficients would be reduced.

In conclusion, we demonstrated the feasibility of using the muscle deformation signal extracted from real-time ultrasound images to characterize the muscle fatigue. Both the SEMG and muscle deformation signals were used to monitor the muscle fatigue of the biceps brachii under the isometric contraction. The results demonstrated that the thickness of the biceps brachii increased first rapidly then gradually during the process of fatigue with the transition moment at approximately 8 s after the contraction reached 80% MVC. In addition, the torque fluctuation due to the failure to maintain the required contraction level could be observed in the SMG signals, while neither the transition phenomenon nor the torque fluctuation behavior could be observed in the SEMG parameters (RMS and MDF), which changed linearly with the time during the experiment period. The results suggest that the combination of the muscle deformation signal and SEMG parameters may give more comprehensive information for the fatigue assessment. The potential applications of the muscle deformation monitoring of fatigue need to be further confirmed with more experiments on subjects with different gender, age, and pathological conditions.

ACKNOWLEDGEMENTS

This work was partially supported by the Research Grants Council of Hong Kong (PolyU 5245/03E), The Hong Kong Polytechnic University (A-PE63, G-U064, G-YE22), and Shanghai Leading Academic Discipline Project (T0102).

REFERENCES

[1] Gandevia SC. Spinal and supraspinal factors in human muscle fatigue. Physiological Reviews. 2001; 81(4): 1725-1789.

[2] Takaishi T, Ono T, Yasuda Y. Relationship between muscle fatigue and oxygen-uptake during cycle ergometer exercise with different ramp slope increments. European Journal of Applied Physiology and Occupational Physiology. 1992; 65: 335-339.

[3] Laube W, Martin J, Tank J, Baevski RM, Schubert E. Heart rate variability - An indicator of the muscle fatigue after physical exercise. Perfusion. 1996; 9: 225-229.

[4] Stackhouse SK, Reisman DS, Binder-Macleod SA. Challenging the role of pH in skeletal muscle fatigue. Physical Therapy. 2001; 12: 1897-1903.

[5] Cooper RG, Edwards RHT, Gibson H, Stokes MJ. Human-muscle fatigue-frequency-dependence of excitation and force generation. Journal of Physiology. 1988; 397: 585-599.

[6] Oka H. Estimation of muscle fatigue by using EMG and muscle stiffness. Engineering in Medicine and Biology Society, 1996. Bridging Disciplines for Biomedicine. Proceedings of the 18th Annual International Conference of the IEEE. 1996; 4: 1449-1450.

[7] De Luca CJ. Myoelectrical manifestations of localized muscular fatigue in humans. Critical Review in Biomedical Engineering 1984; 11: 251-279.

[8] Seghers J, Spaepen A. Muscle fatigue of the elbow flexor muscles during two intermittent exercise protocols with equal mean muscle loading. Clinical Biomechanics. 2004; 19: 24-30.

[9] Jensen BR, Pilegaard M, Sjogaard G. Motor unit recruitment and rate coding in response to fatiguing shoulder abductions and subsequent recovery. European Journal of Applied Physiology. 2000; 83: 190-199.

[10] MacIsaac DT, Parker PA, Englehart KB. A novel approach to localized muscle fatigue assessment. Engineering in Medicine and Biology Society, 2003. Proceedings of the 25th Annual International Conference of the IEEE. 2003; 3: 2487-2490.

[11] MacIsaac DT, Parker PA, Scott RN, Englehart K, Cechetto A. Influence of dynamic factors on myoelectric paramters. IEEE Engineering in Medicine and Biology Magazine. 2001; 20: 84-89.

[12] Kimura T, Hamada T, Watanabe T, Maeda A, Oya T, Moritani T. Mechanomyographic responses in human biceps brachii and soleus during sustained isometric contraction. European Journal of Applied Physiology. 2004; 92: 533-539.

[13] Yoshitake Y, Ue H, Miyazaki M, Moritani T. Assessment of lower-back muscle fatigue using electromyography, mechanomyography, and near-infrared spectroscopy. European Journal of Applied Physiology. 2001; 84: 174-179.

[14] Esposito F, Orizio C, Veicsteinas A. Electromyogram and mechanomyogram changes in fresh and fatigued muscle during sustained contraction in men. European Journal of Applied Physiology. 1998; 78: 494-501.

[15] Hodges PW, Pengel LHM, Herbert RD. Measurement of muscle contraction with ultrasound imaging. Muscle and Nerve. 2003; 27: 682-692.

[16] Zheng YP, Chan MMF, Shi J, Chen X, Huang QH. Sonomyography: Monitoring morphological changes of forearm muscles in actions with the feasibility for the control of powered prosthesis. Medical Engineering and Physics. In print. 2006.

[17] Narici MV, Binzoni T, Hiltbrand E, Fasel J, Terrier F, Cerretelli P. In vivo human gastrocnemius architecture with changing joint angle at rest and during graded isometric contraction. Journal of Physiology. 1996, 496 (1): 287-297.

[18] Fukunaga T, Ichinose Y, Ito M, Kawakami Y, Fukashiro S. Determination of fascicle length and pennation in a contracting human muscle in vivo. Journal of Applied Physiology. 1997; 82: 354-358.

[19] Masamitsu Ito, Yasuo Kawakami, Yoshiho Ichinose. Nonisometric behavior of fascicles during isometric contractions of a human muscle. Journal of Applied Physiology. 1998; 85: 1230-1235.

[20] Maganaris CN, Baltzopoulos V and Sargeant AJ. Repeated contractions alter the geometry of human skeletal muscle. Journal of Applied Physiology. 2002, 93: 2089-2094.

[21] Reeves ND, Maganaris CN, Narici MV. Ultrasonographic assessment of human skeletal muscle size. European Journal of Applied Physiology. 2004, 91: 116-118.

[22] Liber RL. Skeletal muscle structure, function, and plasticity. Lippincott Williams & Wilkins. 2002.

[23] Nordander C, Willner J, Hansson GA, Larsson B, Unge J, Granquist L and Skerfving S. Influence of the subcutaneous fat layer, as measured by ultrasound, skinfold calipers and BMI, on the EMG amplitude. European Journal of Applied Physiology. 2003, 89: 514-519.

[24] McMeeken JM, Beith ID, Newham DJ. The relationship between EMG and change in thickness of transversus abdominis. Clinical Biomechanics. 2004; 19: 337-342.

[25] Mademli L, Arampatzis A. Behaviour of the human gastrocnemius muscle architecture during submaximal isometric fatigue. European Journal of Applied Physiology. 2005; 94: 611-617.

[26] Mademli L, Arampatzis A, Walsh M. Effect of muscle fatigue on the compliance of the gastrocnemius medialis tendon and aponeurosis. Journal of Biomechanics. 2006, 39: 426-434.

[27] Buonocore M, Opasich C, Casale R. Early development of EMG localized muscle fatigue in hand muscles of patients with chronic heart failure. Archives of Physical Medicine and Rehabilitation. 1998; 79: 41-45.

[28] Oberg T. Muscle Fatigue and Calibration of EMG Measurements. J. Electromyogr. Kinesiol. 1996; 5: 239-243.

[29] Kleine BU, Schumann NP, Stegeman DF, Hans-Christoph Scholle. Surface EMG

mapping of the human trapezius muscle: the topography of monopolar and bipolar surface EMG amplitude and spectrum parameters at varied forces and in fatigue. Clinical Neurophysiology. 2000; 111: 686-693.

[30] Cao G, Jiang J, Chen J. An improved object tracking algorithm based on image correlation. IEEE International Symposium on Industrial Electronics. 2004; 1: 598-601.

[31] Montera DA, Rogers SK, Ruck DW, and Oxley ME. Object tracking through adaptive correlation. Optical Engineering. 1994; 33(1): 294-302.

[32] Petrofsky JS, Lind AR. Frequency analysis of the surface electromyogram during sustained isometric conditions. European Journal of Applied Physiology. 1980; 43: 173-182.

[33] Petrofsky JS, Glaser RM, Philips CA, Lind AR, Williams C. Evaluation of the amplitude and frequency components of the surface EMG as an index of muscle fatigue. Ergonomics. 1982; 25: 213-223.

[34] Garland SJ, Enoka RM, Serrano LP, Robinson GA. Behaviour of motor units in human biceps brachii during a submaximal fatiguing contraction. Jounal of Applied Physiology. 1994; 76: 2411-2419.

[35] Henneman E, Somjen G, Carpenter DO. Functional significance of cell size in spinal motorneurons. Journal of Neurophysiology. 1965; 28: 560-580.

[36] Huxley AF. Muscle structure and theories of contraction. Progress in Biophysics and Molecular Biology. 1957; 7: 255-318.

[37] Swammerdam J. Bilia Naturae. 1737. cited by T. Kardel, in Journal of Biomechanics. 1990, 23: 953-965.

[38] Narici M. Human skeletal muscle architecture studied in vivo by non-invasive imaging techniques: functional significance and applications. Journal of Electromyography and Kinesiology. 1999, 9: 97-103.

[39] Nygren AT, Greitz D, Kaijser L. Changes in cross-sectional area in human exercising and non-exercising skeletal muscles. European Journal of Applied Physiology. 2000, 81: 210-213.

[40] Kardel T. Sstensen, Niels geometrical-theory of muscle-contraction (1667) - A reappraisal. Journal of Biomechanics. 1990, 23: 953-965.

[41] Orizio C, Gobbo M, Diemont B, Esposito F, and Veicsteinas A. The surface mechanomyogram as a tool to describe the influence of fatigue on biceps brachii motor unit activation strategy. Historical basis and novel evidence. European Journal of Applied Physiology. 2003, 90: 326-336.

Figure Captions

Fig. 1 The experimental setup for the measurement of muscle fatigue with SMG and SEMG. The area labeled with the small rectangle is magnified in the upper-left corner.

Fig. 2 Motion tracking for the ultrasound images using the two dimensional cross-correlation algorithm. (a) The image taken at the moment when the torque first reached 80% MVC and (b) the image taken when the torque started to decrease below 80% MVC. Two rectangular blocks were selected on the upper and lower boundaries of the cross-sectional image of the biceps brachii, respectively.

Fig. 3 The changes of the SEMG parameters and the muscle deformation during the process of fatigue for a typical trial of a subject. (a) The change of the SEMG RMS normalized by the value of the first data point; (b) the change of SEMG MDF , (c) the change of muscle deformation. Linear regression was used in (a) and (b) to obtain the changing rates of SEMG RMS and MDF. For (c) the muscle deformation, two deformation rates were defined, namely initial muscle deformation rate representing the initial fast thickness change and steady muscle deformation rate representing the slow thickness change after the initial phase. The cross point of the two linear regression lines was defined as the critical time. The circled region indicates that the subject could not maintain the assigned torque any more due to fatigue and the torque value started to fluctuate.

Fig. 4 The mean change rates of SEMG parameters of the 8 subjects calculated from the results of 3 trials. (a) The mean change rate of the normalized RMS of different subjects; (b) the mean change rate of MDF of different subjects. The overall means of all the subjects' change rates of the normalized RMS and MDF were given by the last bars in (a) and (b), respectively. The error bars of the individual results represent the SD of the 3 trials. The errors bars of the overall means represent the SD of the 8 subjects.

Fig. 5 The mean muscle deformation for the 8 individual subjects at 20 s after contraction at 80% MVC, which was calculated from the 3 trials. Their error bars indicate the SD of the 3 trials. The overall mean muscle deformation for the 8 subjects' was given by the last bar with its error bar representing the SD of the values of the 8 subjects.

Fig. 6 The mean parameters of SMG for the 8 subjects calculated from 3 trials. (a) Initial muscle deformation rate; (b) steady muscle deformation rate; and (c) critical time. The overall means of parameters calculated for the 8 subjects are shown in the last bars in (a) to (c), respectively. The error bars of the individual results represent the SD of the 3 trials, and the errors bars of the overall means represent the SD of the values of the 8 subjects.

Figures

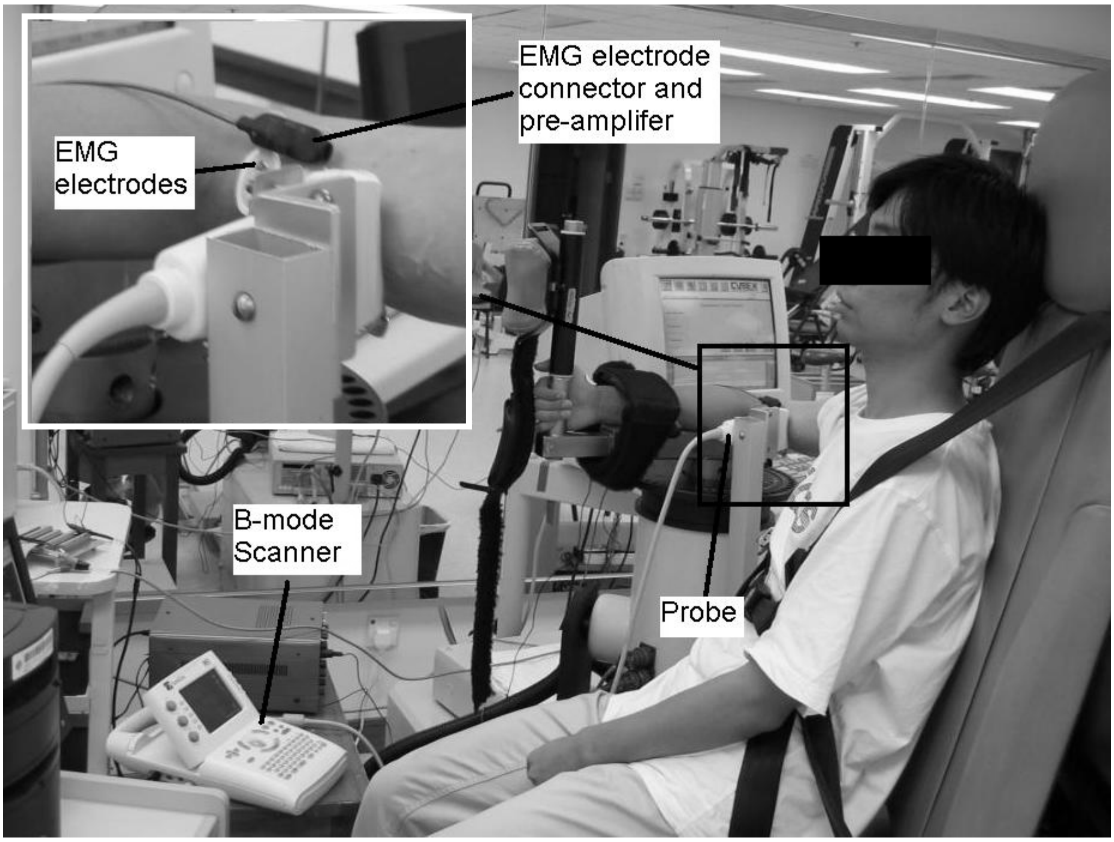

Fig. 1

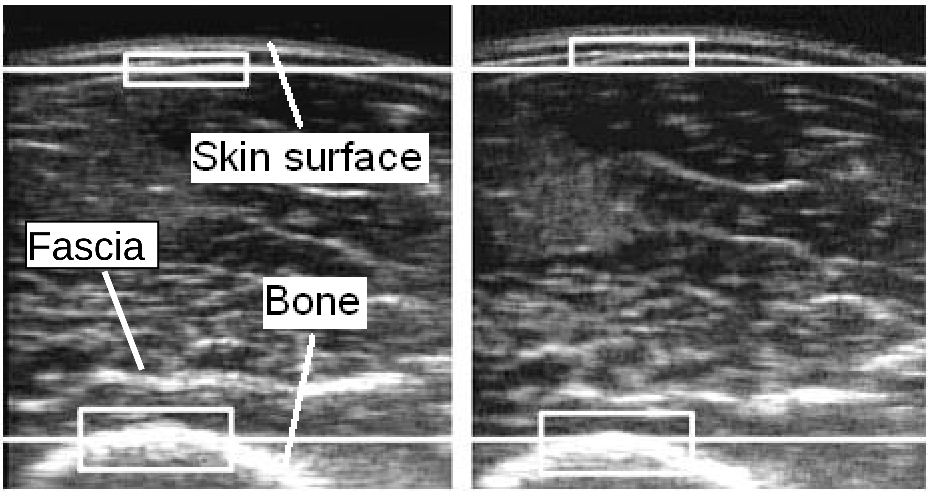

(a) (b)

Fig. 2

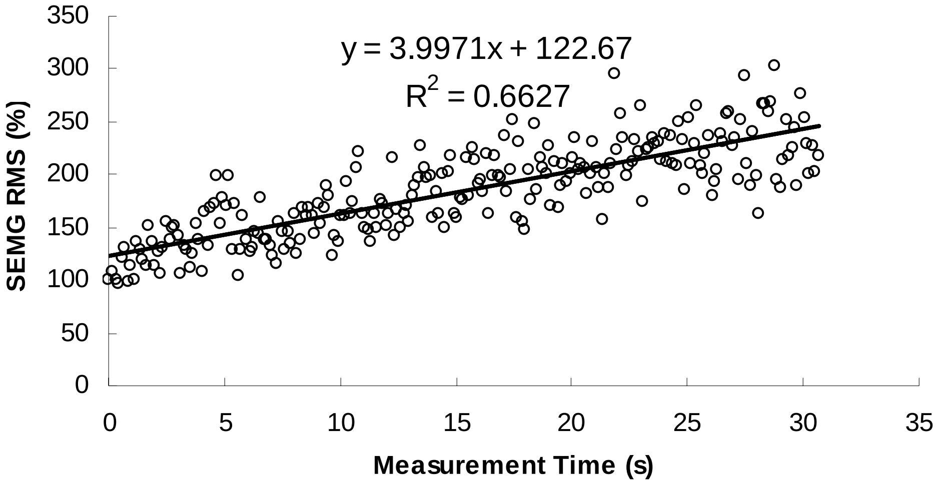
y = 3.9971x + 122.67
R2 = 0.6627
SEMG RMS (%)
Measurement Time (s)
0
50
100
150
200
250
300
350
0
5
10
15
20
25
30
35

(a)

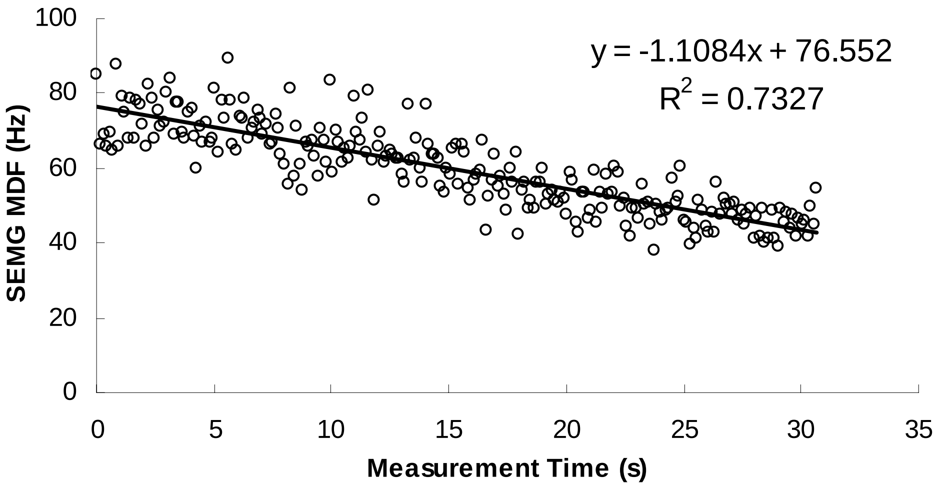
y = -1.1084x + 76.552
R2 = 0.7327
SEMG MDF (Hz)
Measurement Time (s)
0
20
40
60
80
100
0
5
10
15
20
25
30
35

(b)

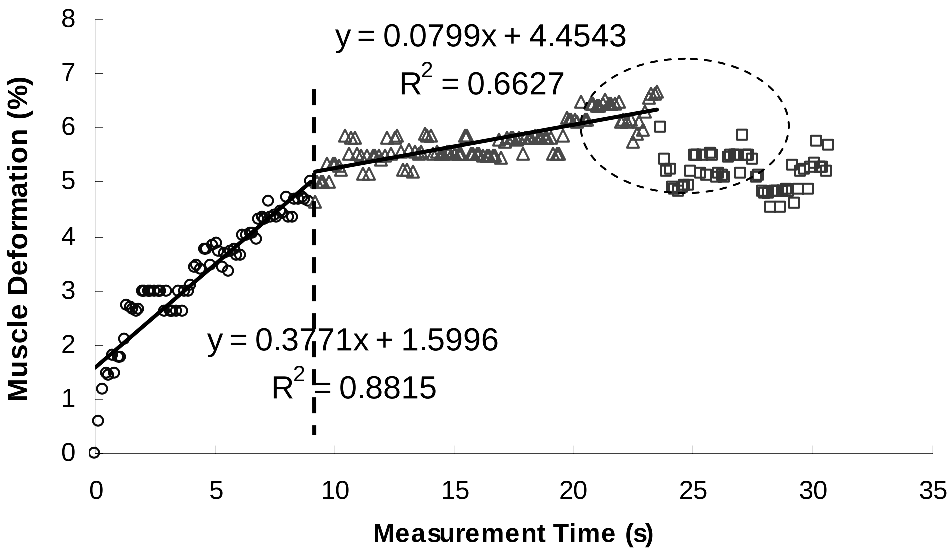
y = 0.0799x + 4.4543
R2 = 0.6627
y = 0.3771x + 1.5996
R2 = 0.8815
Muscle Deformation (%)
Measurement Time (s)
0
1
2
3
4
5
6
7
8
0
5
10
15
20
25
30
35

(c)

Fig. 3

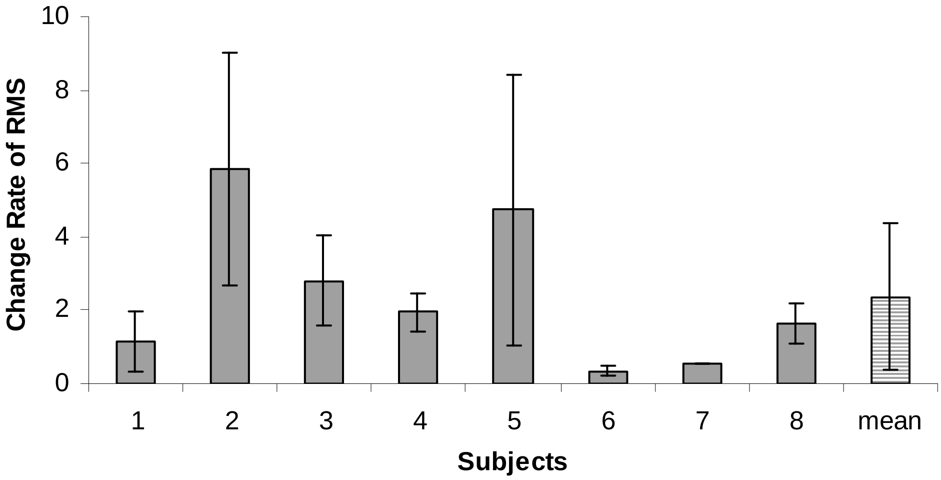

10
8
6
4
2
0
Change Rate of RMS
1
2
3
4
5
6
7
8
mean
Subjects

(a)

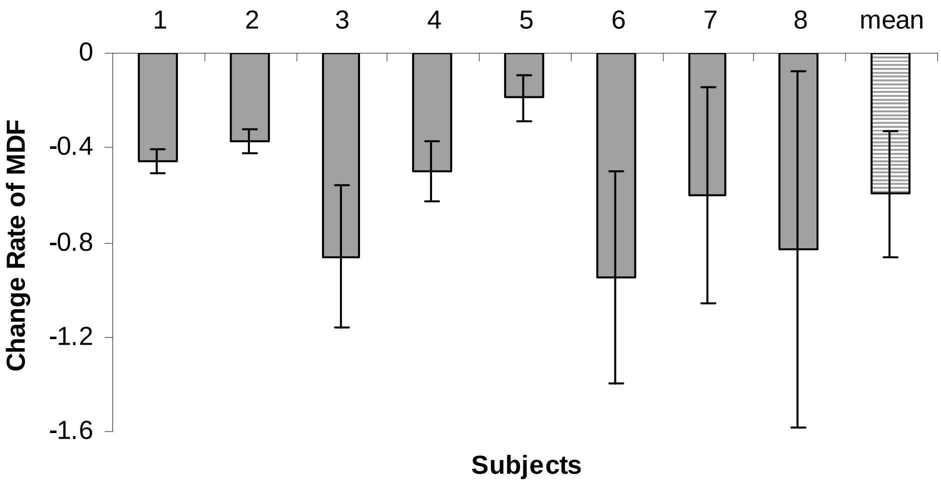

1
2
3
4
5
6
7
8
mean
0
-0.4
-0.8
-1.2
-1.6
Change Rate of MDF
Subjects

(b)

Fig. 4

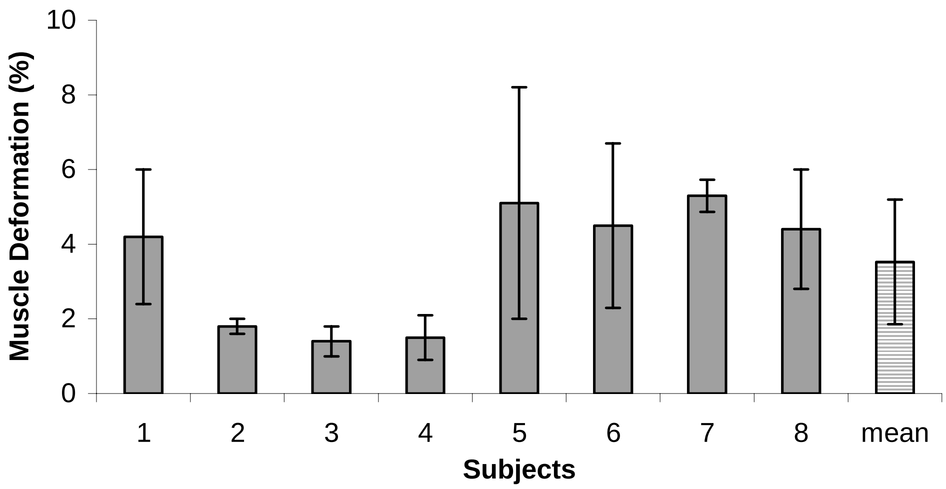

Fig. 5

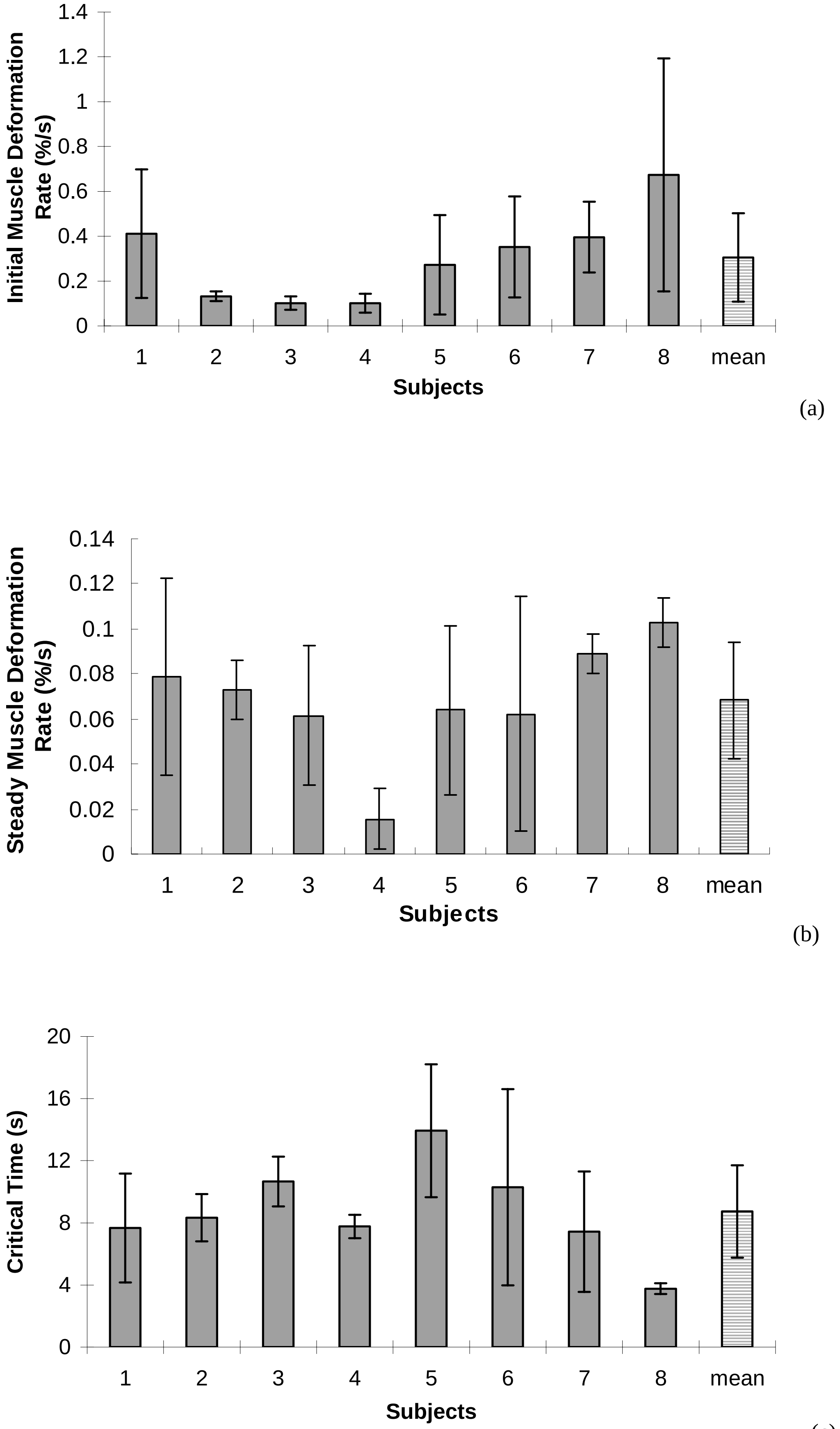
Initial Muscle Deformation Rate (%/s)
0
0.2
0.4
0.6
0.8
1
1.2
1.4
1
2
3
4
5
6
7
8
mean
Subjects
(a)
Steady Muscle Deformation Rate (%/s)
0
0.02
0.04
0.06
0.08
0.1
0.12
0.14
1
2
3
4
5
6
7
8
mean
Subjects
(b)
Critical Time (s)
0
4
8
12
16
20
1
2
3
4
5
6
7
8
mean
Subjects
(c)

Fig. 6